Measured adaptive matching performance of a MIMO terminal with user effects

Vasilev, Ivaylo; Plicanic, Vanja; Tian, Ruiyuan; Lau, Buon Kiong

Published in:
IEEE Antennas and Wireless Propagation Letters

DOI:
10.1109/LAWP.2013.2295681

2013

Document Version:
Peer reviewed version (aka post-print)

Measured Adaptive Matching Performance of a MIMO Terminal with User Effects

Ivaylo Vasilev, *Student Member, IEEE*, Vanja Plicanic, *Member, IEEE*, Ruiyuan Tian, *Member, IEEE*, and Buon Kiong Lau, *Senior Member, IEEE*

***Abstract*—Absorption and impedance mismatch due to the proximity of a user as well as certain propagation channel characteristics can severely degrade the multiple-input multiple-output (MIMO) performance of multi-antenna terminals in real usage scenarios. In this context, we investigated the potential of adaptive impedance matching (AIM) to mitigate performance degradation from these effects based on channel measurements involving a terminal prototype in three user scenarios and two propagation environments. First, optimal AIM state for the terminal in a given user-channel setup was found by post-processing the measured channels. The optimal state was then experimentally verified with two Maury Microwave mechanical tuners. The results show that by employing AIM instead of 50Ω termination, the average capacity is increased by up to 25%. Moreover, the observed capacity gains can be partly explained by physical mechanisms underlying the propagation conditions. Furthermore, the achieved gains with real tuners are only marginally affected by the tuners' actual insertion losses, estimated to be 0.1-0.7 dB. Therefore, we conclude that AIM can be a viable solution to enhance MIMO terminal performance.**

***Index Terms*— Impedance matching, multipath channel, MIMO, channel capacity.**

I. Introduction

ADAPTIVE impedance matching (AIM) has been proposed as a solution for counteracting the detuning of terminal antennas due to proximity of a user or other objects (see e.g., [1]-[3]). The initial work focused on single-antenna systems and the enhancement of received power using AIM. However, multi-antenna based multiple-input multiple-output (MIMO) technology has in recent years received tremendous interest in the wireless communications community, thanks to its ability to offer high data rates and increased link reliability at no increase in power consumption or spectrum usage [4]. As opposed to the single-antenna case, multi-antenna terminals face more challenging design problems: 1) multi-antenna elements distributed within a compact volume increase the likelihood of the antenna elements being detuned by a user; 2) the MIMO performance of multi-antennas (e.g., channel capacity) does not only depend on the received power, but also on correlation, which is a function of the antenna patterns and propagation channel characteristics [4]; and 3) a multiport AIM can influence the matching and coupling coefficients as well as the impedance bandwidth, which in turn affect the received power and correlation in a given channel [4].

In [5], it is shown that received power and correlation of two closely spaced dipole antennas can be individually optimized using uncoupled AIM. Later results indicate that optimizing capacity of dual-dipoles for a given propagation channel using uncoupled AIM involves a trade-off between power and correlation [4], [6]. The effectiveness of AIM to compensate for user-induced performance degradations is studied with respect to antenna parameters of dual-antenna terminals in [7] and [8], underlining conditions for AIM to provide high performance gains. However, these two studies were based on combining simulated or measured patterns with ideal AIM and uniform 3D multipath channel.

Recently, the benefits of AIM were evaluated for a dual-band, dual-antenna terminal based on measured channels [9]. Capacity gains of up to 44% were recorded. However, the measurement campaign considered only one user scenario and an indoor environment. Moreover, lossless AIM networks were added in post-processing and no actual tuners were used.

In the context, this letter provides a substantial extension to the initial work in [9] with more comprehensive and realistic user-channel setups, involving: 1) one- and two-hand grips, each with a half-body phantom, and a reference free-space case, 2) indoor and outdoor environments. Hence, the results provide a detailed picture on the potential benefits of AIM to both researchers and practitioners. Further, we experimentally verified the AIM results obtained from post-processing using real tuners and also identified the mechanisms underlying the achieved AIM gains in different user-channel setups.

II. Measurements Setup and Evaluation Method

A. Terminal Antennas and User Scenarios

The MIMO mobile terminal prototype used in this study is identical in design to the one used in [9] and comprises two compact dual-band inverted-F antennas (IFAs) operating at a low (0.8-0.85 GHz) and a high (2.3-2.4 GHz) frequency band with a maximum reflection coefficient of -6 dB over the bands. The minimum isolations are 5.8 dB and 22 dB for the low and high bands, respectively. The frequency bands were chosen to be close to existing cellular bands, to ensure similar

Manuscript received October 15, 2013. This work was supported in part by VINNOVA under grant no. 2009-02969, and in part by Vetenskapsrådet under grant no. 2010-468.

I. Vasilev and B. K. Lau are with the Department of Electrical and Information Technology, Lund University, 221 00 Lund, Sweden (e-mail: {Ivaylo.Vasilev, Buon_Kiong.Lau}@eit.lth.se).

V. Plicanic is with the Network Technology Laboratory, Sony Mobile Communications AB, 221 88 Lund, Sweden (email: Vanja.Plicanic Samuelsson@sonymobile.com).

R. Tian was with the Department of Electrical and Information Technology, Lund University, 221 00 Lund, Sweden. He is now with Nokia Corporation, 021 50, Espoo, Finland (email: Ruiyuan.Tian@nokia.com).

antenna and propagation channel properties, without having to deal with interference and licensing issues. The receive antennas (Rx) were the terminal antennas. One-hand (OH) and two-hand (TH) user scenarios involving a half-body human phantom and IndexSAR hand phantom(s) holding the terminal in a standing posture (see Fig. 1) represented two common usage cases. The exact positions of the fingers in the OH case closely followed the detailed grip study in [10], whereas those of the TH case followed the grip style in [9]. A free-space (FS) scenario, without the phantom body and hands, was used as a reference case. To ease comparison, the height of the terminal was maintained at around 1.2 m in all three cases.

(a) (b)

Fig. 1. Channel measurement receiver setup – (a) indoor in one-hand mode; (b) outdoor in two hands mode and Maury MT982EU30 tuner.

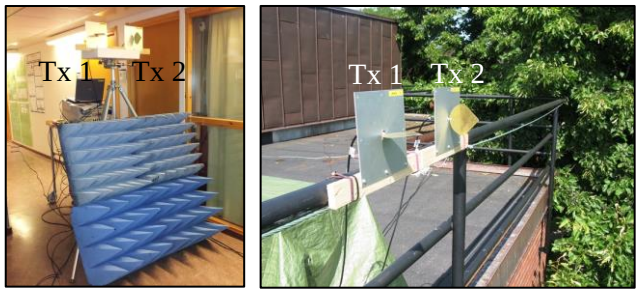

(a) (b)

Fig. 2. Channel measurement transmitter setup – (a) indoor; (b) outdoor.

The transmit antennas (Tx) were two wideband monopole antennas of one wavelength (λ) spacing at 0.8 GHz. The ground planes were positioned vertically at a height of 1.85 m from the floor level in the indoor environment and 8 m from the ground level for the outdoor environment (see Fig. 2).

B. Channel Measurements

The block diagram of the experimental setup is given in Fig. 3. Parts 1_A and 1_B represent the four-port vector network analyzer (VNA) used to measure the four-port S-parameter representation of the 2 × 2 MIMO channel. The intermediate frequency bandwidth (IFBW) of the VNA was set to 2 kHz, and an averaging over 20 snapshots was directly done by the instrument. Both the low and the high frequency bands were measured with a 5 kHz resolution. Part 2 describes the impedance matching networks, which are included in the study either by: 1) post-processing measured channels with ideal matching networks, each consisting of a short-circuit stub (length L_S) and a transmission line (length L_T) [7]; or 2) directly connecting two Maury Microwave MT982EU30 7 mm tuners [11] (see Fig. 1(b)) between the two antennas and two ports of the VNA. Both ideal and real matching networks can achieve a wide range of matching states on the entire Smith chart, including all the states required in this study.

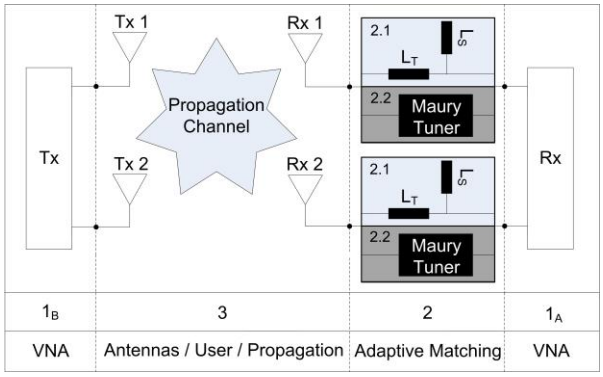

Fig. 3. Channel measurement block diagram.

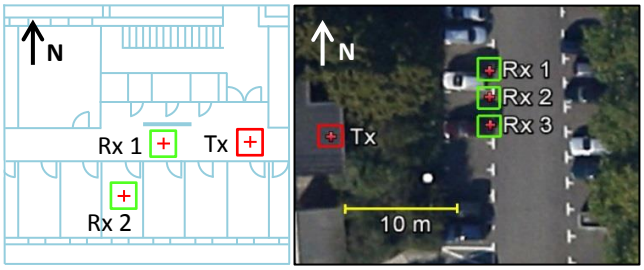

(a) (b)

Fig. 4. Measurement setup of (a) indoor scenario and (b) outdoor scenario (no car was present at the time of measurement).

Due to the low switching speed of the mechanical tuners (~40 sec/state), the study with the tuners was limited to verifying a subset of results obtained by post-processing the measured channels with the ideal tuners (Configuration 2.1 in Fig. 3). For the verification, 10 states were selected per port based on the results from post-processing, giving 100 states per Rx location. In addition, the real tuner measurement was also aimed at evaluating the actual insertion loss of the tuners.

Part 3 represents the Tx and Rx in their respective operating scenarios (e.g., in proximity of user), as well as the propagation channel in between. Two distinct environments were measured. The indoor environment was a corridor with offices at both sides (first floor, South-wing of E-building, Lund University, see Fig. 4(a)). The Tx was fixed at the same position while the Rx was measured in two locations, each over a grid of five measurement points at 1 λ spacing (at 800 MHz) to average out small-scale fading per location (along with frequency realizations). The phantom was facing east. The outdoor environment was a parking lot outside the E-building, with the Rx measured at three locations in the parking lot and the Tx placed on the rooftop of the adjacent building (see Fig. 4(b)). The phantom was facing west. Due to space constraint, we limit our discussions to Rx location 2 (Rx 2) for both the indoor and outdoor cases, since these results are representative of the entire measurement campaign.

III. Results and Discussion

To evaluate system performance, MIMO capacity was calculated using the measured channels (either with ideal AIM networks in post-processing or with directly connected Maury tuners). These calculations were executed over a bandwidth of 10 MHz, which is the standard downlink bandwidth of LTE Bands 13 and 14. To ensure good accuracy in the capacity calculation in the presence of channel estimation error, the

reference signal-to-noise ratio (SNR) was set as 10 dB. This is because the measured average SNRs for all setups were at least 10 dB higher than the evaluation SNR. To compare between the different user-channel setups, the measured indoor and outdoor channels were normalized by the average channel power in the respective FS scenarios (post-processed without AIM). This enables the experimental verification of simulation results as well as the estimation of losses due to the use of real tuners relative to ideal AIM. Capacity for each matching state was evaluated and the one giving the maximum capacity over all states was considered as the optimal state.

A. Adaptive Matching Results with Ideal Matching Networks

Table 1 shows the average capacity without AIM, capacity gain with AIM, power gain and eigenvalue dispersion (ED) gain [9] for 9 different cases at low and high frequency bands (LB, HB) in both indoor (In) and outdoor (Out) environments.

TABLE I

CAPACITY GAIN, POWER GAIN AND EIGENVALUE DISPERSION (ED) FOR RX POSITION 2 FOR INDOOR (IN) AND OUTDOOR (OUT) CASES

Case	Average Capacity – no AIM [bits/s/Hz]	Capacity Gain with AIM		ED Gain [dB]	Power Gain [dB]
		[bits/s/Hz]	[%]		
In-LB-FS	5.3	0.1	1	-0.6	0.3
In-LB-OH	1.8	0.2	13	-0.2	1
In-LB-TH	3.4	0.8	25	0.7	2.1
Out-LB-FS	5.3	0.1	1	-0.5	0.3
Out-LB-OH	5.7	0.4	6.5	~0	1
Out-LB-TH	4.0	0.7	18	0.2	1.6
Out-HB-FS	4.7	~0	0.6	~0	0.1
Out-HB-OH	6.7	0.1	1	0.1	0.2
Out-HB-TH	3.6	0.3	8	0.2	0.7

Comparing between In-LB-FS and In-LB-TH, the user hands are observed to cause a severe capacity degradation of 1.9 bits/s/Hz (without AIM). However, applying AIM leads to a promising capacity gain of 0.8 bits/s/Hz (or 25%). It is noted that the capacity gain of 25% for the indoor TH scenario is lower than the 44% gain obtained in [9]. This is attributed to fabrication tolerance (i.e., another prototype of the same design was used) as well as the presence of the half-body phantom. It was confirmed in full-wave simulation using CST Microwave Studio that the body slightly reduces the mismatch caused by the hands, which decreases achievable capacity gain from AIM. Moreover, due to the use of narrowband matching, the average capacity gain will decrease if a larger system bandwidth (>10 MHz) is considered [12]. Consistent to the observation in [9], the dominant source of improvement is higher received power (2.1 dB) rather than improved channel richness from antenna pattern variations due to AIM (as measured by ED gain of 0.7 dB). Nevertheless, the modest ED gain indicates that the optimal matching state for capacity necessitates a tradeoff between achieving higher received power and lower correlation, rather than merely maximizing received power by minimizing impedance mismatch. These observations hold also for other cases except for In-LB-FS and Out-LB-FS, where only minor received power improvements were obtained as the terminal was well matched for FS operation. Overall, the results in Table 1 project a few trends. Due to the relative position between the hand and the terminal antennas (in OH only one element was in the palm of the hand, whereas in TH both elements were covered by the hands), the mismatch and therefore capacity gains in the OH cases are significantly lower than those in the TH cases (6.5-13% for LB-OH vs. 18-25% for LB-TH). Furthermore, since the user effects were less severe in the high band (also observed in [9]), the capacity gain is only up to 8% for these cases. The somewhat surprising result of higher average capacity of the OH cases than the FS cases in the outdoor scenario can be explained by the use of FS case in channel normalization, where different orientations of the terminal between the FS and OH cases in a given propagation channel had resulted in significantly larger received power in the OH cases. In addition, the AIM capacity gains in the low band are lower in the outdoor setups relative to the indoor setups. The physical mechanism underlying this capacity difference will be elaborated in Section III-C.

B. Experimental Verification Using Maury Tuners

Since the evaluation in Section III-A was performed with ideal AIM in post-processing, it is important to verify the results in representative cases with measurements using real tuners. Moreover, an estimation of the actual tuner insertion loss during operation is needed to determine if the achieved AIM gain is still attractive when the loss is considered.

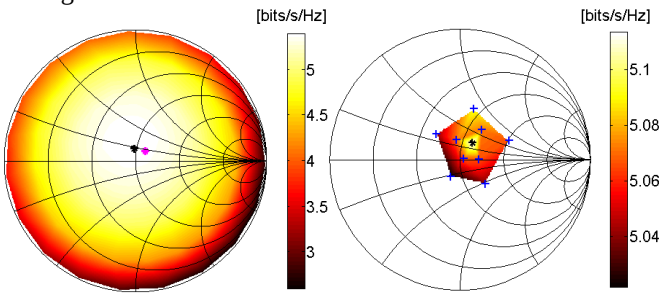

Fig. 5. Average capacity for In-LB-FS over matching states at port 2 - (a) ideal tuners; (b) Maury tuners. Markers indicate antenna Z_{IN}^* (magenta star), optimal state (black star) and 10 Maury tuner states (blue cross).

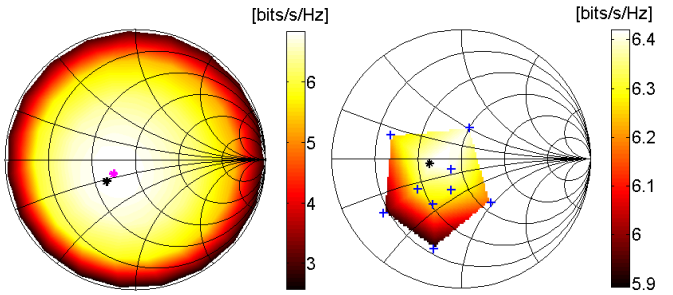

Fig. 6. Average capacity for Out-HB-OH over matching states at port 2 - (a) ideal tuners; (b) Maury tuners. Markers indicate antenna Z_{IN}^* (magenta star), optimal state (black star) and 10 Maury tuner states (blue cross).

Figures 5 and 6 compare the average capacity over the matching states on the Smith chart (of port 2) for the ideal vs. real tuners in In-LB-FS and Out-HB-OH, respectively. To ease the visualization of results, it is assumed that port 1 has been optimally matched for capacity. The real tuner states were chosen in the vicinity of the optimum state for capacity as predicted by the ideal tuners. The capacity between the 10 states in Figs. 5(b) and 6(b) were obtained by interpolation. In each setup, it is observed that the chosen states of the tuner

measurements capture the global maximum of the capacity, and the optimal state agrees well with that of the ideal tuners.

The Maury tuner loss was estimated for each of these two user-channel setups by comparing the average channel gains at the optimal state for the ideal tuners and the real tuners. The losses were estimated to be 0.1 dB and 0.7 dB for In-LB-FS and Out-HB-OH, respectively, which agrees well with the specified tuner insertion losses (at the 50 Ω state) of up to 0.4 dB in the range 2-8 GHz [11]. It is noted that the slightly higher 0.7 dB loss (vs. 0.4 dB) in the Out-HB-OH setup can be attributed to the optimal state being located away from the 50 Ω state, which increases insertion loss [13].

Taking into consideration the tuner losses discussed here and the results in Table 1, it can be concluded that real tuners will largely offset the received power gain from AIM in all cases except In-LB-TH and Out-LB-TH. In particular, the FS cases will likely suffer from lower capacity due to the insertion loss than if no tuner is used. Nevertheless, it may still be attractive to achieve an improved performance in realistic user scenarios at the price of poorer performance in the idealized FS setup. Moreover, although the Maury tuners with low insertion loss are large and impractical for terminal integration, compact integrated AIM circuits with low losses, e.g., those based on MEMS [14], are becoming more common.

C. Physical Mechanisms for Adaptive Matching Gains

In this subsection, we describe in detail the physical mechanism behind the lower AIM capacity gain in the outdoor scenario as compared to the indoor scenario. In essence, the difference is attributed to the directional characteristics of the propagation channel. In particular, the indoor scenario with the Rx at location 2 presents a rich multipath environment, due to the absence of line-of-sight (LOS) between the Tx and Rx and multiple scattering objects in vicinity. Such a channel can be represented by the uniform 3D angular power spectrum (APS), with incoming waves randomly distributed in direction and polarization. Therefore, the spatially uniform indoor channels render the AIM performance insensitive to the orientation of the terminals and dependent only on the change in the *global* behavior in the antenna patterns from AIM.

On the other hand, the outdoor scenario is designed to be LOS, in which case, a directional channel (i.e., with narrow angular spread) can be expected from the dominant LOS direction. Consequently, the AIM performance depends on the extent to which the AIM changes the antenna patterns within the illuminated region (i.e., *local* behavior) to achieve maximum capacity, relative to the change in the overall pattern (*global* behavior) in the uniform channel case.

Below, the OH user scenario is used to illustrate different AIM capacity gains due to different directional properties of the channel. For this user case, the antenna patterns for both ports were obtained from CST Microwave Studio. Assuming lossless and uncorrelated transmit antennas, the Kronecker model was used to synthesize the channel based on the total efficiency and pattern correlation of the terminal in the OH case [15]. The average capacity was then obtained from multiple realizations of the channel. Likewise, the optimal capacity with AIM for the uniform channel was calculated using the same procedure, except that the matching state was optimized for maximum capacity. The capacity gain was 6%.

For the outdoor scenario, a K-factor of 8.3 is obtained for the OH case at Rx location 2, which indicates a directional APS. This scenario can be modeled by a Gaussian APS with 15° angular spread. The capacity without AIM (50 Ω) can then be calculated by combining the antenna patterns with the Gaussian APS, based on the mean effective gain and correlation at the ports [15]. The capacity with AIM was then obtained using the same procedure, but for the optimal matching state. Depending on the mean angle of the Gaussian APS, the capacity gain for the outdoor case is calculated to vary between 2-15%, confirming that directionality of the channel can account for differences obtained in the AIM gain.

IV. Conclusions

The focus of this work was to experimentally evaluate the performance benefits of AIM under representative user and channel conditions. It was found that AIM offers significant capacity gains in cases involving a user by achieving higher received power and/or lower correlation, even when the insertion loss of real tuners is accounted for. Moreover, the directional characteristics of the channel are shown to have a significant influence on the performance gain from AIM.

References

[1] J. P. Phillips, E. L. Krenz, A. A. Efanov, R. M. Alameh, and R. L. Scheer, "Sensor-driven adaptive counterpoise antenna system," US Patent 6 657 595, Dec. 2, 2003.

[2] K. R. Boyle, Y. Yuan, and L. P. Ligthart, "Analysis of mobile phone atennna impedance variations with user proximity", *IEEE Trans. Antennas Propag.*, vol. 55, no. 2, pp. 364-372, Feb. 2007.

[3] S. M. Ali et al., "Dynamic measurement of complex impedance in real-time for smart handset applications," *IEEE Trans. Microw. Theory Tech.*, vol. 61, no. 9, Sep. 2013.

[4] B. K. Lau, "Multiple antenna terminals," in *MIMO: From Theory to Implementation*, C. Oestges, A. Sibille, and A. Zanella, Eds. San Diego: Academic Press, 2011, pp. 267-298.

[5] J. B. Andersen and B. K. Lau, "On closely coupled dipoles in a random field," *IEEE Antennas Wireless Propag. Lett*., vol. 5, pp. 73-75, 2006.

[6] R. Mohammadkhani and J. S. Thompson, "Adaptive uncoupled termination for coupled arrays in MIMO systems," *IEEE Trans. Antennas Propag.*, vol. 61, no. 8, pp. 4284-4295, Aug. 2013.

[7] I. Vasilev, E. Foroozanfard, and B. K. Lau, "Adaptive impedance matching performance of MIMO terminals with different bandwidth and isolation properties in realistic user scenarios," in *Proc. Europ. Conf. Antennas Propag.*, Gothenburg, Sweden, Apr. 2013, pp. 2516-2520.

[8] I. Vasilev, V. Plicanic, and B. K. Lau, "On user effect compensation of MIMO terminals with adaptive impedance matching," *in Proc. IEEE Int. Symp. Antennas Propag.*, Orlando, USA, Jul. 2013, pp. 174-175.

[9] V. Plicanic, I. Vasilev, R. Tian, and B. K. Lau, "Capacity maximisation of handheld MIMO terminal with adaptive matching in indoor environment," *IET Electron. Lett.*, vol. 47, no. 16, pp. 900-901,2011.

[10] M. Pelosi et al.,"A grip study for talk and data modes in mobile phones," *IEEE Trans. Antennas Propag.*, vol. 57, no. 4, pp. 856-865, Apr. 2009.

[11] [Online]. Available: http://www.maurymw.com/

[12] B. K. Lau, J. B. Andersen, G. Kristensson and A. F. Molisch, "Impact of matching network on bandiwdth of compact antenna arrays," *IEEE Trans. Antennas Propag.*, vol. 54, no. 11, pp. 3225-3238, Nov. 2006.

[13] R. Valkonen, C. Icheln, and P. Vainikainen, "Power dissipation in mobile antenna tuning circuits under varying impedance conditions," *IEEE Antennas Wireless Propag. Lett.*, vol. 11, pp. 37-40, 2012.

[14] R. Valkonen et al., "Frequency-reconfigurable mobile terminal antenna with MEMS switches," *in Proc. 4th Europ. Conf. Antennas Propag*, Barcelona, Spain, Apr. 2010, pp. 1-5.

[15] R. Tian, B. K. Lau, and Z. Ying, "Multiplexing efficiency of MIMO antennas in arbitrary propagation scenarios," in *Proc. 6th Europ. Conf. Antennas Propag.*, Prague, Czech Republic, Mar. 2012.